Pupil Tracking and Spiking Neural Network Modeling of Horizontal Nystagmus

Samyak Jain
sam.j.272009@gmail.com

1. Introduction

1.1 Background

Nystagmus is a congenital or acquired ocular-motor condition of involuntary, often rhythmic eye movements [1], [8]. The oscillations may be horizontal, vertical, or torsional and vary in waveform, frequency, and amplitude, sometimes reducing visual acuity or causing oscillopsia. Jerk nystagmus has a slow phase with a rapid corrective movement, while pendular nystagmus is more nearly sinusoidal [2]. It can arise from instability in the systems that stabilize gaze, including the vestibulo-ocular reflex, the gaze-holding integrator, brainstem nuclei, and the cerebellum [1], [8].

1.2 Problem

Nystagmus intensity changes with gaze direction, convergence, attention, and fatigue [2], so quantitative measurement is important for characterizing the condition and evaluating interventions. Video-oculography gives objective measures of waveform, amplitude, and frequency that supplement clinical examination [5], [7], and computational models can then test how alternating activity in ocular-motor pathways may generate the oscillations [3]. This study used video-based pupil tracking across several viewing and physiological conditions, together with a two-population neural model, to examine a possible mechanism for the observed rhythms.

2. Methods

2.1 Experimental Recordings

Videos were recorded with a stationary camera at 1920 × 1080 pixels and about 30 frames/s. One participant with nystagmus was recorded under the conditions in Table 1, and one without nystagmus served as a negative control (Experiment 0). Experiment 1 was the straight-ahead reference and the comparison for Experiments 6–8, since separate pre-screen, rested, and without-glasses recordings were unavailable.

TABLE 1
EXPERIMENTAL CONDITIONS AND THEIR PURPOSES

EXPERIMENT	CONDITION	PURPOSE
0	Participant without nystagmus	Negative control
1	Straight-ahead gaze	Baseline nystagmus
2L, 2R, 2U, 2D	Left, right, up, and down gaze	Gaze dependence
3	Reading text	Functional impact
4N, 4F	Near and far fixation	Accommodation effect
5M, 5N	Morning and evening recordings	Fatigue and time-of-day effects
6	After 3 hours of screen use	Visual strain effect
7	After 2 hours of physical activity	Physiological state effect
8	With glasses	Optical correction effect
9	Viewing moving black-and-white stripes	Optokinetic response

2.2 Pupil Tracking

Pupils were extracted with Python and OpenCV: eye regions were converted to grayscale, smoothed, and thresholded, and candidate contours were scored by size, shape, darkness, and proximity to the previous position (Fig. 1). Small facial movements were corrected with sparse Lucas–Kanade optical flow, and pupil coordinates were mapped into a stabilized facial frame. Frames without a confident detection were treated as missing; tracking error is the percentage of such frames (Fig. 2).

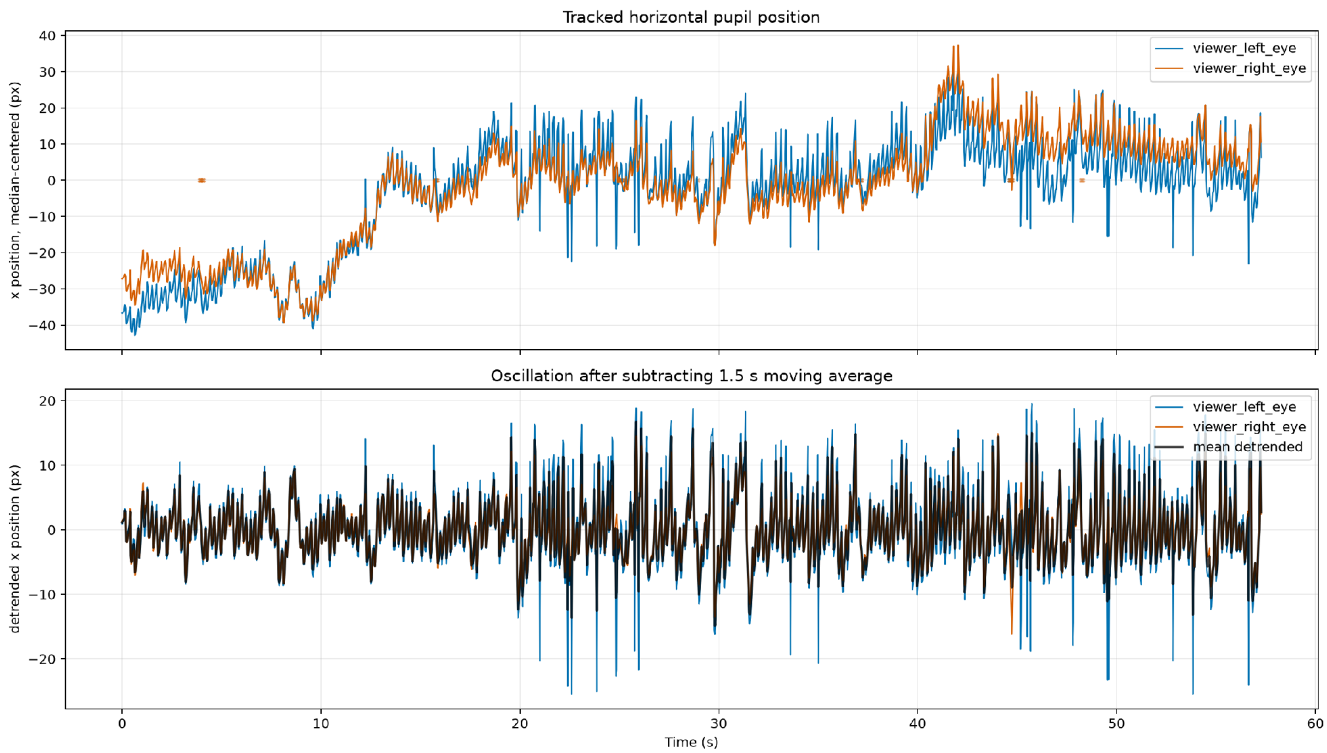

Fig. 1. Representative OpenCV tracking in Experiment 1. Top: median-centered left- and right-pupil positions. Bottom: signals after removing a 1.5-s moving average, with the mean detrended binocular trace in black.

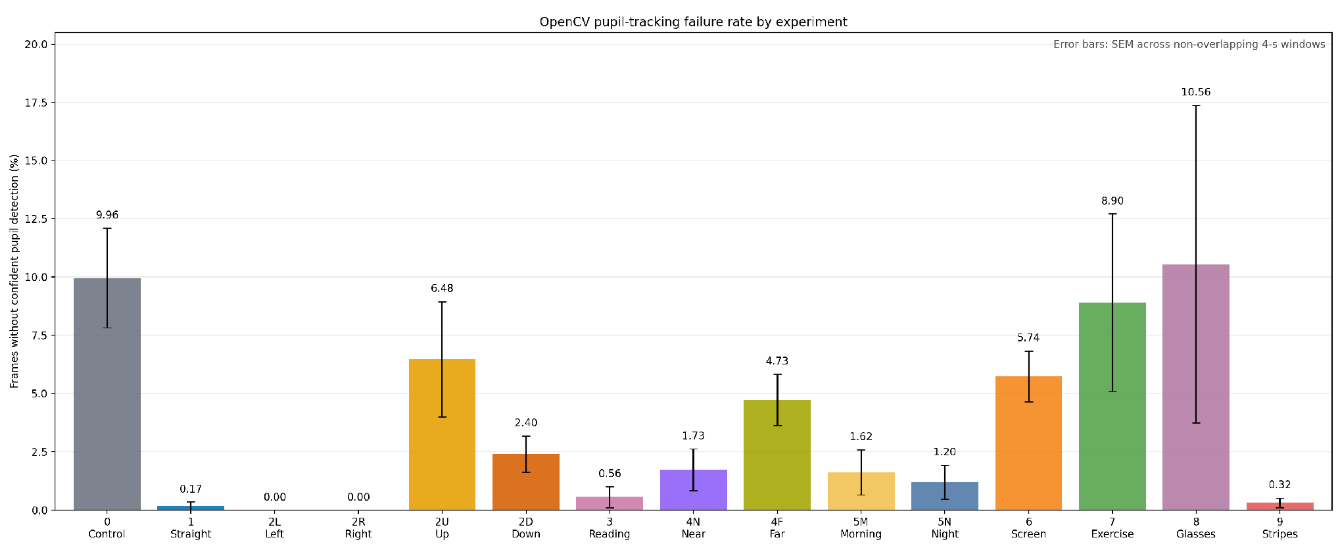

Fig. 2. OpenCV pupil-tracking failure rate by condition (percentage of frames without a confident detection). Error bars show the standard error across 4-s windows.

2.3 Oscillation Analysis

Stabilized horizontal traces were band-pass filtered from 0.5 to 8 Hz with a fourth-order zero-phase Butterworth filter, and a binocular trace was formed by averaging the eyes. Dominant frequency came from Welch spectra and left–right coherence; a rhythm was accepted when coherence was at least 0.35 and its spectral score at least 6 dB above background, otherwise reported as not detected (ND). Amplitude was the 95th-minus-5th-percentile displacement, measured in non-overlapping 4-s windows.

2.4 Neural Oscillator Model

A two-population model tested whether alternating activity in rightward- and leftward-preferring populations, with reciprocal inhibition and adaptation, could reproduce the eye movements. Their dynamics were

$$\begin{aligned} \tau_r \frac{du_R}{dt} &= -u_R - g\,r_L - b\,a_R + I \\ \tau_r \frac{du_L}{dt} &= -u_L - g\,r_R - b\,a_L + I \\ \tau_a \frac{da_R}{dt} &= -a_R + r_R \\ \tau_a \frac{da_L}{dt} &= -a_L + r_L \end{aligned} \tag{1}$$

with rectified population rates

$$r_R = \max(0,\, u_R), \quad r_L = \max(0,\, u_I \tag{2}$$

where u_R, u_L are population activities, a_R, a_L adaptation variables, g reciprocal inhibition, b adaptation strength, and I tonic input. An adaptive leaky integrate-and-fire version used 120 neurons per population, and the difference between the smoothed rates drove a first-order ocular plant,

$$\tau_e \frac{dx}{dt} = -x + K\,(r_R - r_L) \tag{3}$$

Experiment 1 calibrated baseline frequency and pixel gain. To represent conditions, the baseline output x_0 was rescaled by a fitted gate, timescale, and gain,

$$x_c(t) = q_c\, G_c\, x_0\!\left(\frac{t}{s_c}\right) \tag{4}$$

with the gate zero for ND recordings, the timescale setting frequency, and the gain setting amplitude. Because these were fit to the same recordings, the results are in-sample calibration rather than independent prediction.

3. Results

3.1 Measured Pupil Oscillations

Coherent oscillation was detected in 11 of 15 recordings; none met the criteria for the control (Experiment 0), left gaze (2L), up gaze (2U), or far fixation (4F). The straight-ahead baseline (Experiment 1) measured 4.10 Hz and 3.14% of inter-pupil distance. Similar frequencies occurred for down gaze (4.30 Hz), near fixation (3.96 Hz), morning and evening (3.85 and 3.99 Hz), screen exposure (4.23 Hz), and moving stripes (3.77 Hz); slower rhythms occurred for right gaze (0.73 Hz), reading (0.71 Hz), exercise (1.26 Hz), and glasses (2.60 Hz). The largest amplitudes were in the morning (4.46%), reading (4.05%), and evening (4.03%), and the smallest was right gaze (0.43%) (Fig. 3).

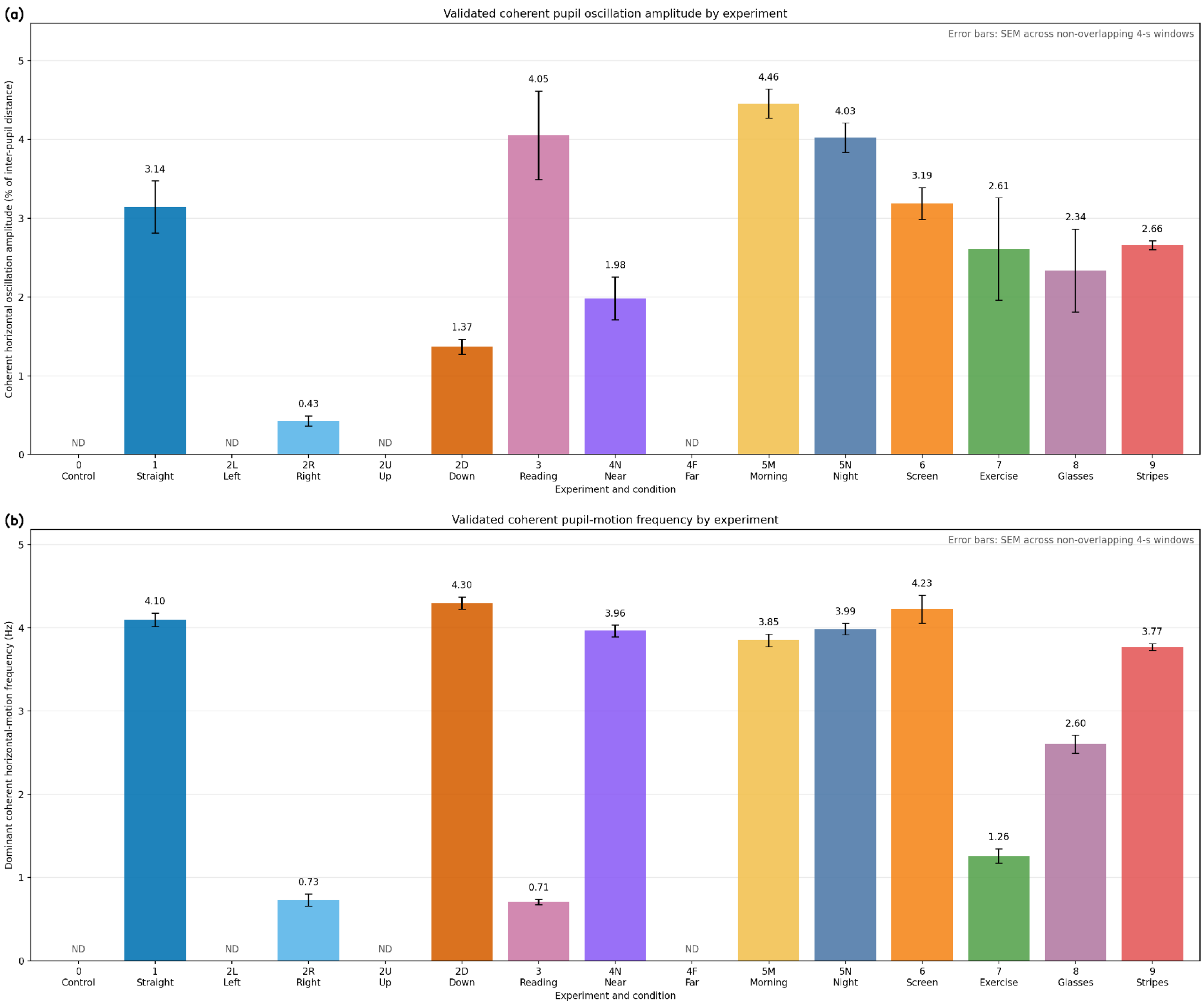

Fig. 3. Measured pupil-oscillation amplitude (a) and dominant frequency (b) by condition. Amplitude is a percentage of inter-pupil distance; error bars show the standard error across 4-s windows. ND indicates no detected oscillation.

3.2 Condition-Aware Model Fit

The model reproduced the detected or ND state of every recording, with amplitude set by the condition gain. Fitted frequencies stayed within two standard errors of measurement (mean absolute error 0.081 Hz across the ten non-baseline detected recordings), and mean phase-aligned waveform correlation rose from 0.357 for the fixed baseline model to 0.663 (Fig. 4). The best matches were Experiment 8 ($r = 0.87$), 9 (0.83), 6 (0.82), and 1 (0.81), while reading was weakest (0.11), consistent with its nonstationary movements.

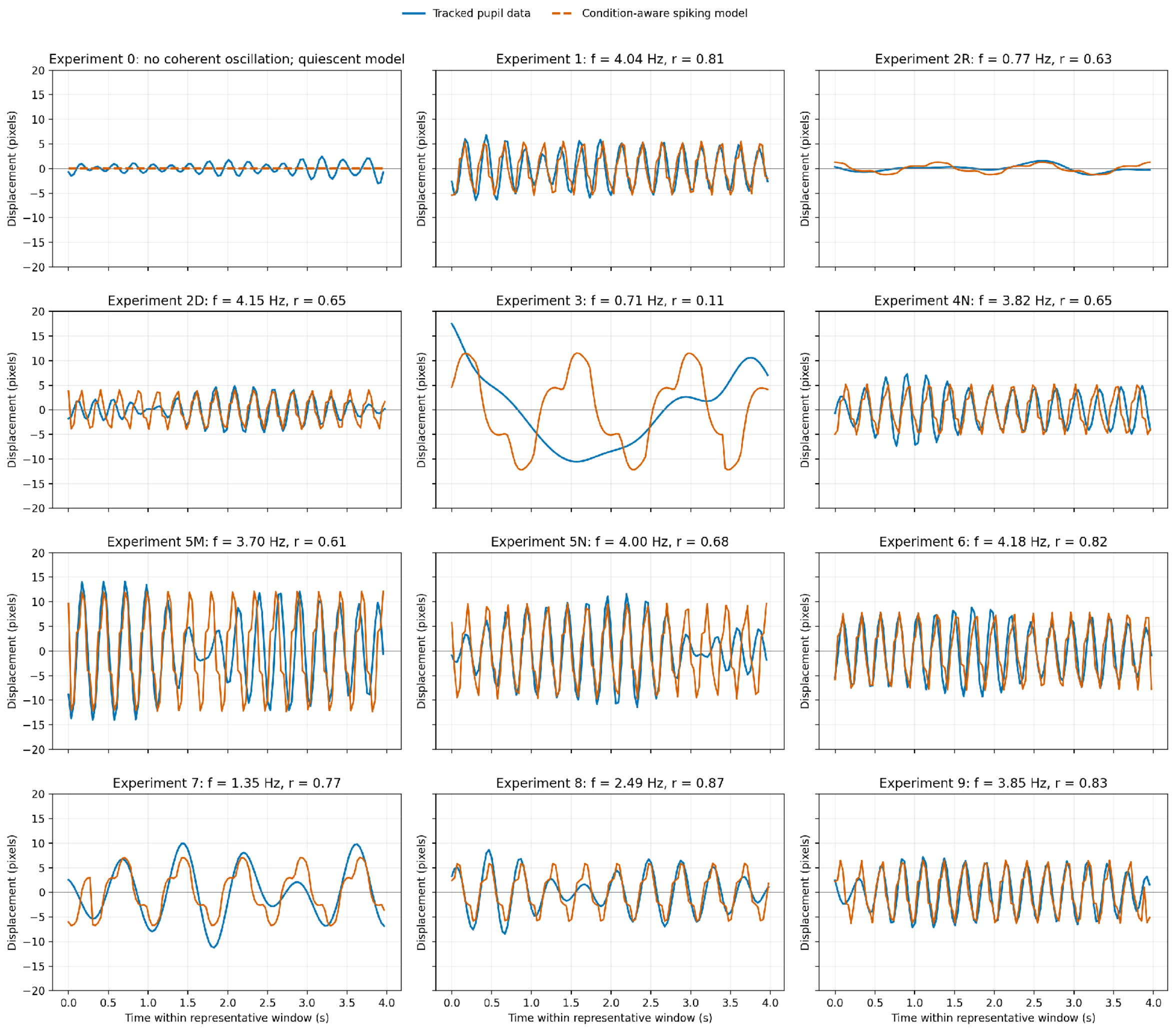

Fig. 4. Tracked pupil displacement (blue) and condition-aware model fits (orange), all at the same vertical scale. Experiment 0 shows the control and quiescent model; f and r are given for detected oscillations.

3.3 Spiking-Network Activity

The spiking network produced alternating population activity that generated oscillatory eye output (Fig. 5). Experiment 1 gave a 4.04-Hz rhythm (r = 0.81), and applying the slower Experiment 7 timescale gave a 1.35-Hz rhythm (r = 0.77), showing that one mechanism can span timescales.

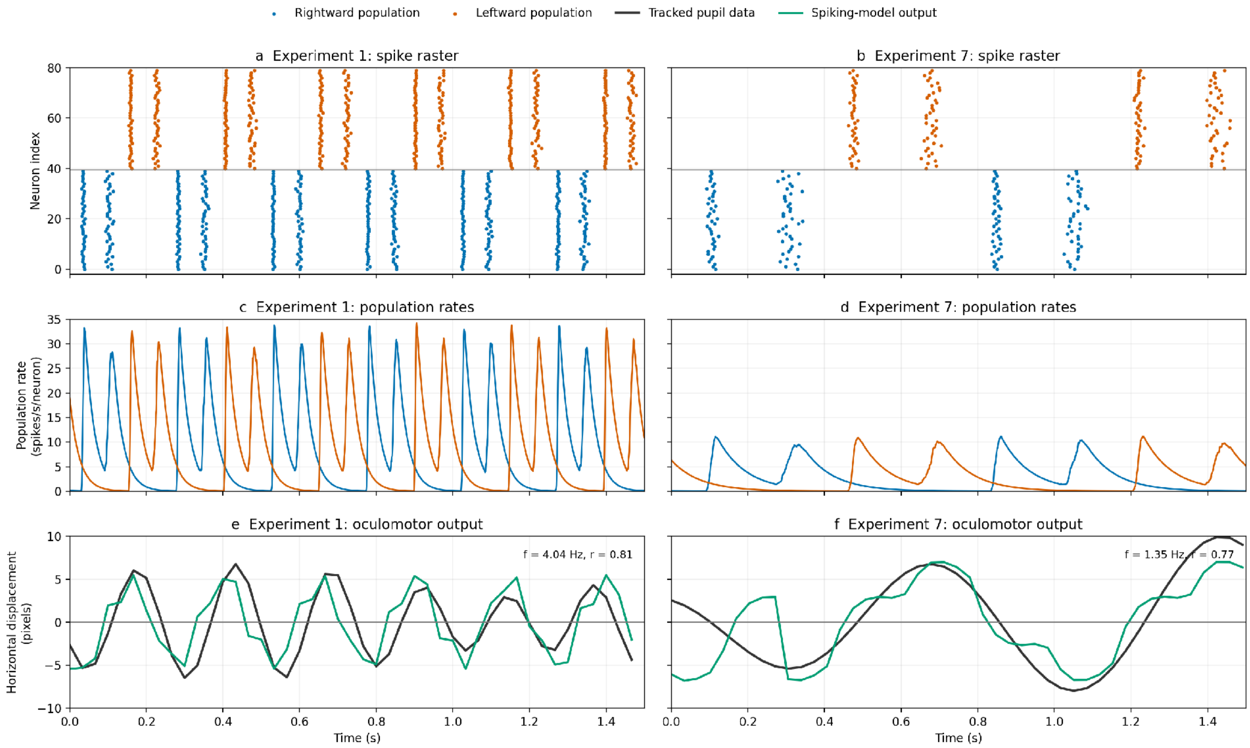

Fig. 5. Spiking-network simulations for Experiments 1 and 7. Alternating population activity drives the modeled eye displacement, giving a 4.04-Hz rhythm (Exp. 1) and a 1.35-Hz rhythm (Exp. 7), correlating with tracked motion at r = 0.81 and r = 0.77.

Increasing reciprocal inhibition drove a transition from balanced to alternating activity (Fig. 6). At g = 0.4 the rates were balanced and output stayed below the control threshold; oscillation appeared at g = 0.8, and at g = 2.0 the model matched the Experiment 1 amplitude and produced a 4.0-Hz rhythm, near the measured 4.10 Hz.

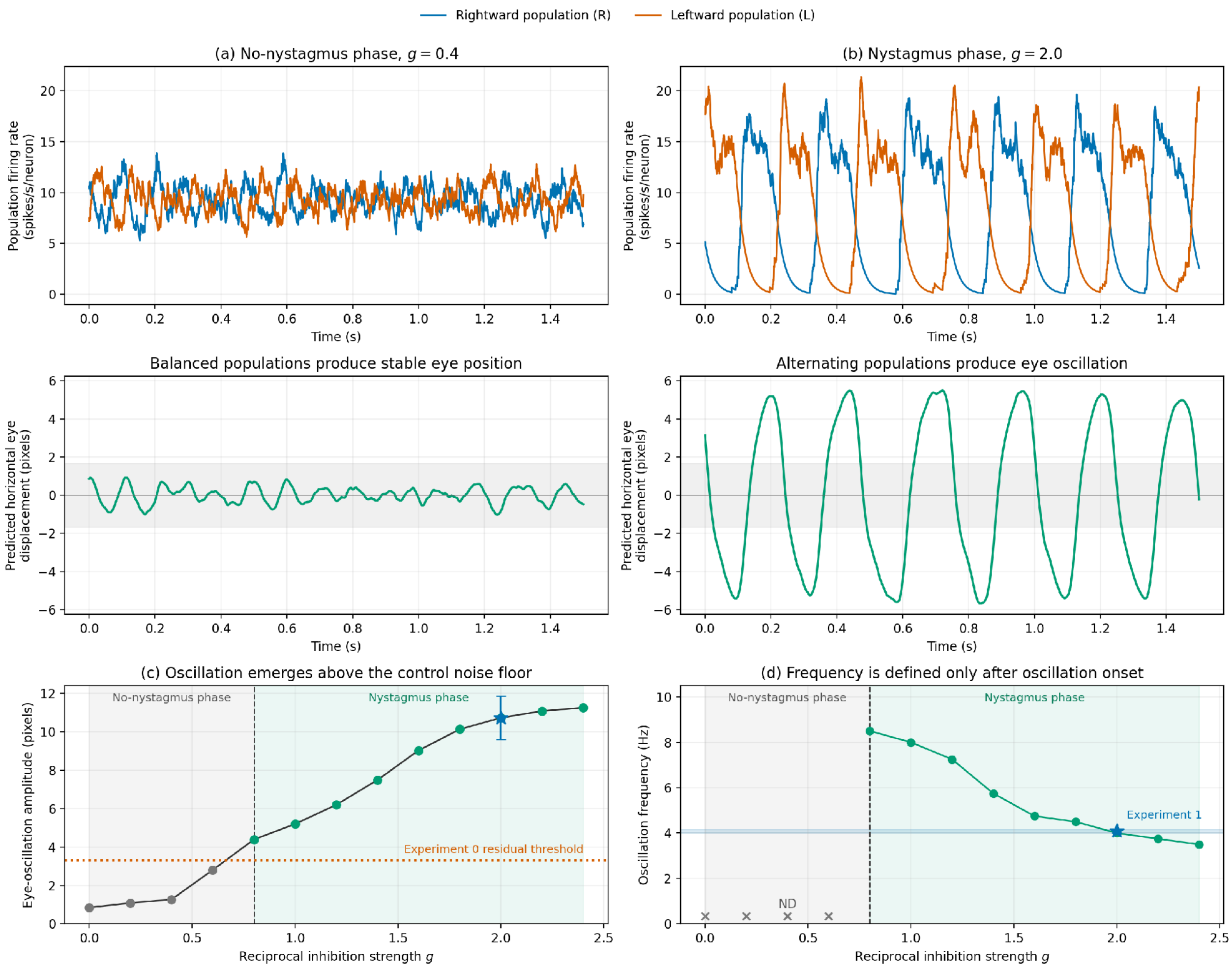

Fig. 6. Transition from no detectable nystagmus to nystagmus-like output. Below g = 0.8 the populations stay balanced and output stays within the control range; at g = 2.0 the simulated amplitude and frequency match Experiment 1.

4. Conclusion

Video-based pupil tracking quantified condition-dependent changes in horizontal nystagmus. The participant with nystagmus showed a 4.10-Hz baseline rhythm, absent in the control, and amplitude and frequency varied with gaze direction, fixation distance, reading, time of day, screen exposure, exercise, optical correction, and moving stimulation, so nystagmus is not a fixed oscillation and should be evaluated under more than one condition.

The two-population model gave a plausible mechanism: alternating population activity produced oscillation while balanced activity produced stable position, and increasing reciprocal inhibition moved the spiking network from a no-detection state to a nystagmus-like state that matched Experiment 1. Limitations include the small number of participants, pixel-based measurement, and condition parameters fit to the same data; future work should add participants, calibrated eye-position measurement, repeated sessions, and independent validation.

References

[1] R. V. Abadi, “Mechanisms underlying nystagmus,” J. R. Soc. Med., vol. 95, no. 5, pp. 231–234, 2002, doi: 10.1177/014107680209500504.
[2] R. V. Abadi and A. Bjerre, “Motor and sensory characteristics of infantile nystagmus,” Br. J. Ophthalmol., vol. 86, no. 10, pp. 1152–1160, 2002, doi: 10.1136/bjo.86.10.1152.
[3] L. F. Dell’Osso, “Biologically relevant models of infantile nystagmus syndrome: The requirement for behavioral ocular motor system models,” Semin. Ophthalmol., vol. 21, no. 2, pp. 71–77, 2006, doi: 10.1080/08820530600613795.

[4] V. L. N. Fu et al., “Visual acuity development of children with infantile nystagmus syndrome,” Invest. Ophthalmol. Vis. Sci., vol. 52, no. 3, pp. 1404–1411, 2011, doi: 10.1167/iovs.09-4686.
[5] M. Tekavcic Pompe, A. Liasis, and R. Hertle, “Visual electrodiagnostics and eye movement recording: World Society of Pediatric Ophthalmology and Strabismus consensus statement,” Indian J. Ophthalmol., vol. 67, no. 1, pp. 23–30, 2019, doi: 10.4103/ijo.IJO_1103_18.
[6] M. D. Richards and A. Wong, “Infantile nystagmus syndrome: Clinical characteristics, current theories of pathogenesis, diagnosis, and management,” Can. J. Ophthalmol., vol. 50, no. 6, pp. 400–408, 2015, doi: 10.1016/j.jcjo.2015.07.010.
[7] J.-R. Rizzo et al., “Eye movement recordings: Practical applications in neurology,” Semin. Neurol., vol. 39, no. 6, pp. 775–784, 2019, doi: 10.1055/s-0039-1698742.
[8] M. Strupp et al., “Central oculomotor disturbances and nystagmus: A window into the brainstem and cerebellum,” Dtsch. Arztebl. Int., vol. 108, no. 12, pp. 197–204, 2011, doi: 10.3238/arztebl.2011.0197.